Reduced-Order Aggregate Model for Large-scale Converters with Inhomogeneous Initial Conditions in DC Microgrids

Wang, Rui; Sun, Qiuye; Tu, Pengfei; Xiao, Jianfeng; Gui, Yonghao; Peng, Wang

Published in:
I E E E Transactions on Energy Conversion

DOI (link to publication from Publisher):
10.1109/TEC.2021.3050434

Publication date:
2021

Document Version
Accepted author manuscript, peer reviewed version

Reduced-Order Aggregate Model for Large-scale Converters with Inhomogeneous Initial Conditions in DC Microgrids

Rui Wang, *Student Member, IEEE*, Qiuye Sun, *Senior Member, IEEE*, Pengfei Tu, *Member, IEEE*, Jianfang Xiao, *Member, IEEE*, Yonghao Gui, *Senior Member, IEEE,* Peng Wang, *Fellow, IEEE*

***Abstract*—In practical microgrids, the inhomogeneous initial values are widely appeared due to soft-starting operation. If traditional model order reduction approaches are applied, the input-output maps error between the original system and reduced-order system is large. To address this problem, this paper proposes a reduced-order aggregate model based on balanced truncation approach to provide the preprocessing approach for the real-time simulation of large-scale converters with inhomogeneous initial conditions in DC microgrid. Firstly, the standard linear time-invariant model with inhomogeneous initial conditions is established through non-leader multiagents concept. To end this, it is convenient for scholars to build complex system modeling with switched topology. Furthermore, the full system is divided into two components, *i.e.,* the unforced component with non-trivial initial conditions and forced component with null initial conditions. Moreover, this paper presents an aggregated approach that involves independent reducing component responses and combining reducing component responses. Based on this, the input-output maps error is reduced. Then, the approximated error estimate of the reduced-order aggregate model regarding large-scale converters in DC microgrid is first provided, which provides prior knowledge and theoretical basis for DC microgrid designers. Finally, the simulation results illustrate the accuracy of the proposed approach.**

***Index Terms*—large-scale converters, inhomogeneous initial conditions, reduced-order aggregate model, balanced truncation approach.**

I. Introduction

HIGH penetration of renewable energy sources has increased the number of power electronics converters in DC microgrids [1]. Scalable models with limited computational complexity are critical to model and analyze the dynamic characteristics of large numbers of converters in the real-time simulation aspect [2]. Although model order reduction approaches have been widely used for the system consisting of large-scale converters, the initial values requirement is always ignored, or it is avoided through making the restrictive assumption that the initial values are zero [3]-[4]. Due to the soft-starting operation, there is no doubt that the system initial values are not always zero [5]. If initial values are wrongly ignored, the input-output maps error will be large, which is difficult for real-time simulators to adopt this reduced order model. To address this problem, this paper proposes a reduced-order aggregate model based on balanced truncation approach to provide the preprocessing approach for the real-time simulation of large-scale converters with inhomogeneous initial conditions in DC microgrids.

For power system consisting of large-scale converters, there are three main equivalent modeling approaches, *i.e.*, impedance-based approach, transfer function based approach and state-space based approach [6]-[11]. Therein, the impedance-based approach paid more attentions on interactive stability assessment, which was not suitable for real-time simulation [6]-[7]. Although the transfer function based approach was applied to real-time simulation, it was difficult for the system with numerous converters to obtain the full order model [8]. To sum up, the state-space based approach became an advisable choice for real-time simulation [9]-[11]. For AC microgrids, the state-space function model of the converters without voltage/current cascaded controller was established in [9]. Moreover, the full order state-space function model regarding the small-scale microgrid was built in [10]. For DC microgrids, the state-space function model of the converters with plug-and-play (PnP) regulator and $V-I$ droop controller was built in [11]. Nevertheless, for numerous converters, the high order state-space function model should be established [8]. Detailed representations of large-scale converters yielded more accurate conclusions but demand high calculative burden, calling thus for the rapid development regarding model order reduction approaches [12].

Model order reduction approaches regarding state-space function were widely researched in the real-time simulation aspect [12]-[26]. From the timescale and physical property viewpoint, the singular perturbation approach was proposed to reduce model order [12]. Although this approach was much intuitive to construct in dynamical models consisting of multiple timescales, the detailed physical representation of small-perturbation parameter ε was difficult for scholars to

This work was supported by National Key Research and Development Program of China (2018YFA0702200), National Natural Science Foundation of China (U20A20190, 62073065). (*Corresponding authors: Qiuye Sun*)

Rui Wang is with the College of Information Science and Engineering in Northeastern University, Liaoning, 110819, China. (e-mail: 1610232@stu.neu.edu.cn.)

Qiuye Sun is with the State Key Laboratory of Synthetical Automation for Process Industries, Northeastern University, Shenyang 110819, China, and also with the School of Information Science and Engineering, Northeastern University, Shenyang 110819, China (e-mail: sunqiuye@ise.neu.edu.cn.)

Pengfei Tu and Peng Wang are with the Nanyang Technological University, 637141, Singapore. (e-mail: ptu002@e.ntu.edu.sg; epwang@ntu.edu.sg.)

Jianfang Xiao is with the Newcastle University in Singapore, 639798, Singapore. (E-mail: jfxiao@ntu.edu.sg).

Yonghao Gui is with the Automation & Control Section at the Dept. Electronic Systems, Aalborg University, 9220 Aalborg, Denmark. (e-mail: yg@es.aau.dk.)

obtain [13]. To sum up, another series of mathematic model order reduction approaches were proposed in turn, such as slow-coherency method, Krylov-subspace method, Gramian-based method and so on [14]-[16]. Additionally, model order reduction approaches were applied to different fields [17]-[26]. For wireless power transfer systems, dynamic phasor-based reduced-order models were proposed in [17]. For fast power system simulations, an adaptive nonlinear model reduction approach was proposed in [18]. For Li-Ion batteries, reduced-order electrochemical models were presented in [19]. For complex wind farms, a trajectory piecewise-linear approach was applied to reduce model order in [20]. For large sparse small-signal electromechanical stability power systems, the system parameter preserving model order reduction approach was designed in [21]. For islanded droop-controlled microgrids, inter-inverter oscillations based reduced-order models were proposed in [22]. For the DC microgrid with large-scale converters, a reduced-order method based on quadratic eigenvalue problem (QEP) theorem was proposed in [23]-[24], which effectively simplified the stability analysis. Moreover, a power-flow model based on Kron reduction was derived to analyze the power-flow of the large-scale DC microgrid, thus obtaining the analytic existence condition for feasible power-flow by using nested interval theorem [25]. Furthermore, one singular perturbation approach was proposed to reduce the model order through multiple timescales [26]. However, the foresaid pieces of literature always ignored initial values or made the restrictive assumption that the initial values were zero. Due to the soft-starting operation, the above assumption will no longer hold, which results in huge input-output response errors based on traditional model order reduction approaches. Since one perfect reduced-order model ought to exist one reduced state-space vector and mimic the simulated input-output response with the desired accuracy while requiring one lower computational burden [12]. To this end, for eliminating the impact of inhomogeneous initial conditions, this paper proposes a reduced-order aggregate model based on balanced truncation approach to provide the preprocessing approach for the real-time simulation of large-scale converters. Undoubtedly, the proposed model order reduction approach can also be extended into other fields, such as AC microgrids, AC/DC hybrid microgrids and so on. The main advantages of this paper are shown as follows:

1) The standard linear time-invariant model with inhomogeneous initial conditions is established through non-leader multiagents concept. Based on this, it is convenient for scholars to build complex system modeling with switched topology or "plug and play" feature;

2) For the foresaid system, the reduced-order aggregate model based on balanced truncation approach is presented to provide preprocessing for the real-time simulation. With these efforts, the errors between the output variables of the full order model and the output variables of the reduced order model are reduced;

3) Utilizing the mathematical theorem, the approximated error estimate of the reduced-order aggregate model regarding large-scale converters is provided in this paper. Based on this, the prior knowledge and theoretical basis can be provided for DC microgrid designers.

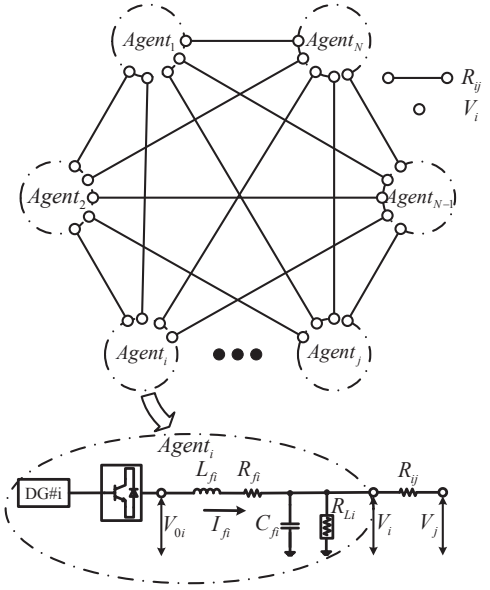

Fig. 1: The topological structure of the dc microgrid consisting of various DGs.

The remainder of this paper is shown as follows. The full-order state-space model based on non-leader multiagent concept is built in Section II, which is consisting of inhomogeneous initial conditions. Furthermore, the reduced-order aggregate model based on balanced truncation approach is proposed to provide preprocessing for the real-time simulation in Section III. And in Section IV, the approximated error estimate of the reduced-order aggregate model regarding large-scale converters is provided through mathematical theorem. In Section V, the simulation results are provided to verify the effectiveness of the proposed reduced-order aggregate model. Finally, the conclusion is given in Section VI.

II. State-space function model of large-scale converters with inhomogeneous initial conditions

The classical topological structure of the DC microgrid consisting of various distributed generators (DGs) is depicted in Fig. 1. Meanwhile, this structure will be changed accordingly to assume the presence of the number of DGs [11]. According to Kirchoff's voltage and current laws, the model of DGs is obtained as follows:

$$C_{fi}\frac{dV_i}{dt} = I_{fi} - \frac{V_i}{R_{Li}} + \sum \frac{V_j - V_i}{R_{ij}} \quad (1)$$

$$L_{fi}\frac{dI_{fi}}{dt} = V_{0i} - V_i - R_{fi}I_{fi} \quad (2)$$

where V_i and V_j represent the interfaced voltage of the i^{th} agent and j^{th} agent, respectively. R_{fi}, L_{fi} and C_{fi} represent the RLC filter of the i^{th} DG, respectively. V_{0i} and I_{fi} represent the output voltage and current of the i^{th} DG, respectively. R_{Li} represents common resistor load. R_{ij} represents the line resistance between the i^{th} agent and the j^{th} agent. Therein, the multiagent concept can be found in AC microgrids [27].

Based on this, the state-space function of the DC microgrid can be obtained as follows:

$$\begin{aligned}\frac{d}{dt}\bar{x}_i(t) &= \bar{A}_{ii}\bar{x}_i(t)+\sum\bar{A}_{ij}\left(\bar{x}_i(t)-\bar{x}_j(t)\right)\\ &\quad +\bar{B}_{ii}\bar{u}_i(t) \qquad (3)\\ \bar{y}_i(t) &= \bar{C}_{ii}\bar{x}_i(t) \qquad (4)\end{aligned}$$

where $\bar{x}_i$, $\bar{u}_i$ and $\bar{y}_i$ are the state variable, input variable and output variable of the i^{th} agent, respectively. Therein, $\bar{x}_i(t)=(V_i,I_{fi})^T$, $\bar{u}_i(t)=V_{0i}$, $\bar{y}_i(t)=m_iI_{fi}$, and m_i is the $V-I$ droop coefficient, which is introduced in the following section. Furthermore, $\bar{A}_{ii}=\left[-\frac{1}{C_{fi}R_{Li}},\frac{1}{C_{fi}};-\frac{1}{L_{fi}},-\frac{R_{fi}}{L_{fi}}\right]$, $\bar{A}_{ij}=\left[-\frac{1}{C_{fi}R_{ij}},0;0,0\right]$, $\bar{B}_{ii}=\left[0,\frac{1}{L_{fi}}\right]^T$ and $\bar{C}_{ii}=[0,m_i]$. The power loss has been reflected through RLC filter circuit R_{fi} and line impedance R_{ij}. To this end, they are embedded in system model. Meanwhile, the influence of branch has been embedded into the system model through R_{ij}. In order to achieve the power sharing among various DGs and stability operation, the zero controller and primary controller are embedded into the interfaced converter, *i.e.*, plug and play (PnP) controller and $V-I$ droop controller [11], [28]. According to the literature [28], the PnP controller is shown as follows:

$$\bar{u}_i(t)=n_{i,1}V_i+n_{i,2}I_{fi}+n_{i,3}\int_0^t\left(V_{ref,i}-V_i\right)dt \qquad (5)$$

where $n_{i,1}$, $n_{i,2}$ and $n_{i,3}$ represent PI controller coefficients of the i^{th} DG, respectively. $V_{ref,i}$ represents the reference voltage of the i^{th} DG. Based on the literature [28], the zero controller is asymptotically stable, if the parameters of the zero controller satisfy the following constraint conditions.

$$\begin{aligned}n_{i,1} &< \left(\sum\frac{1}{R_{ij}}+\frac{1}{R_{Li}}\right)\times\left(R_{fi}-n_{i,2}\right)+1 \qquad (6)\\ n_{i,2} &< \frac{L_{fi}}{C_{fi}}\left(\sum\frac{1}{R_{ij}}+\frac{1}{R_{Li}}\right)+R_{fi} \qquad (7)\\ n_{i,3} &\in \left(0,\left(n_{i,1}-1\right)\left(n_{i,2}-R_{fi}\right)/L_{fi}\right) \qquad (8)\end{aligned}$$

Furthermore, the $V-I$ droop controller is adopted as the primary controller to achieve power sharing among various DGs and voltage regulation. And the detailed $V-I$ droop controller is provided as follows:

$$V_{refi}=V_i^*-m_iI_i \qquad (9)$$

where V_i^* represents the output voltage of the i^{th} DG when unloading. m_i is the $V-I$ droop coefficient of the i^{th} DG, which can be chosen based on the literature [11] to ensure controller asymptotical stability. In order to remove the integral item $n_{i,3}\int_0^t\left(V_{ref,i}-V_i\right)dt$, define $\bar{z}_i(t)=\int_0^t\left(V_{refi}-V_i\right)dt$, $n_i^p=[n_{i,1},n_{i,2}]$, $n_i^i=n_{i,3}$ and $A_i^*=[-1,-m_i]$. To this end, the following function can be provided:

$$\begin{aligned}\bar{u}_i(t) &= n_i^p\bar{x}_i(t)+n_i^i\bar{z}_i(t) \qquad (10)\\ \frac{d}{dt}\bar{z}_i(t) &= A_i^*\bar{x}_i(t)+V_i^* \qquad (11)\end{aligned}$$

According to (3)-(4) and (7)-(8), the total state-space function model of DC microgrid, which is based on non-leader multiagent concept, is estimated as follows

$$\begin{aligned}\dot{x}_i(t) &= \left(A_{ii}+\sum A_{ij}\right)x_i(t)-\sum A_{ij}x_j(t)\\ &\quad +B_{ii}u_i(t) \qquad x_i(0)=x_{i0} \qquad (12)\\ y_i(t) &= C_{ii}x_i(t) \qquad (13)\end{aligned}$$

where $A_{ii}=\begin{bmatrix}\bar{A}_{ii}+\bar{B}_{ii}n_i^p & \bar{B}_{ii}n_i^i\\ A_i^* & 0\end{bmatrix}$, $A_{ij}=\begin{bmatrix}\bar{A}_{ij} & 0_{2*1}\\ 0_{1*2} & 0\end{bmatrix}$, $B_{ii}=\begin{bmatrix}n_i^p\\ n_i^i\end{bmatrix}$, $C_{ii}=\begin{bmatrix}\bar{C}_{ii}\\ 0\end{bmatrix}^T$, $x_i=\left(\bar{x}_i^T(t),\bar{z}_i^T(t)\right)^T$, $u_i=\bar{u}_i$, $y_i=\bar{y}_i$. Thus, the standard linear time-invariant model with inhomogeneous initial conditions is established through non-leader multiagents concept.

Remark 1: Each subsystem can be regarded as one agent. Therein, it is convenient for scholars to obtain the state matrix A_{ii}, input matrix B_{ii} and output matrix C_{ii} for each agent. Furthermore, the coupling relationship between two agents can be reflected through $\sum A_{ij}$. Finally, the overall state-space function is provided through each agent. It is through introducing the non-leader multi-agents concept, that the system modeling process can be easier to understand and operate. Although the modular model look the same, the parameters of the state matrix A_{ii}, input matrix B_{ii} and output matrix C_{ii} for each agent are different. The real system structure, such as common resistor load R_{Li}, RLC filter and so on, is reflected through detailed parameters. For example, the overall load in one DC microgrid is represented as R_{Li}.

Based on this, the full-order state-space function is shown as follows:

$$\begin{aligned}\dot{x}(t) &= Ax(t)+Bu(t) \qquad x(0)=x_0 \qquad (14)\\ y(t) &= Cx(t) \qquad (15)\end{aligned}$$

where $A\in R^{3N\times3N}$, $B\in R^{3N\times N}$, $C\in R^{N\times3N}$, and N represents the number of the DGs in the DC microgrid. If the parameters of the zero and primary controllers satisfy the foresaid constraint conditions, the DC microgrid is asymptotically stable. Due to soft-starting operation, it is impossible in the practical system that $x_0=(V_{i0},I_{fi0},\bar{z}_{i0}(t))^T=(0,0,0)^T$.

Remark 2: Unfortunately, the traditional model order reduction approach is not suitable for the system with $x_0\neq0$, which is shown in (14)-(15). For example, consider the two-dimensional linear time-invariant system with inhomogeneous initial conditions

$$\begin{aligned}\dot{x}(t) &= \begin{bmatrix}-0.5 & 0\\ 0 & -0.5\end{bmatrix}x(t)+\begin{bmatrix}0.01 & 0\\ 0 & 1\end{bmatrix}u(t) \qquad (16)\\ y(t) &= \begin{bmatrix}1 & 0\\ 0 & 1\end{bmatrix}x(t) \qquad x(0)=\begin{bmatrix}1\\ 0\end{bmatrix} \qquad (17)\end{aligned}$$

The Hankel singular values of the system are $\lambda_1=1$, $\lambda_2=0.01$, respectively. Since $\lambda_2\ll\lambda_1$, the one-dimensional reduced order model is provided [16]:

$$\begin{aligned}\dot{x}_r(t) &= -0.5x_r(t)+\begin{bmatrix}0 & 1\end{bmatrix}u(t) \qquad (18)\\ y_r(t) &= \begin{bmatrix}0\\ 1\end{bmatrix}x_r(t) \qquad x_r(0)=0 \qquad (19)\end{aligned}$$

Especially, $\|y(t)-y_r(t)\|_{L_2(0,\infty)}=1$ with trivial input $u=(0,0)^T$ is found through simulation verification, which

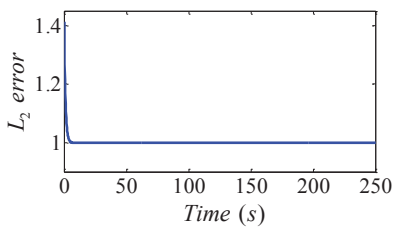

Fig. 2: The error between the output of the full order model and the output of the reduced order model in example.

is shown in Fig. 2. To this end, the norm of the output error between the original system and reduced-order system is constantly equal to the unit, which is not accepted for real-time simulations.

III. Reduced-order aggregate model based on balanced truncation approach

For large-scale converters, it is exorbitantly expensive to apply the resulting mathematical models (14)-(15) with high order to the real-time simulation. To this end, it is advisable to reduce the dimension of large original systems for low computational burden. For the linear state-space systems researched in this paper, the balanced truncation method is superior to the state truncation in terms of approximation error, which is found in the literature [29]. Based on this reason, the balanced truncation approach is chosen in this paper to achieve model order reduction. In this section, two model order reduction approaches without/with inhomogeneous initial conditions are introduced for large input-output systems, which are based on balanced truncation.

A. Model order reduction approach with homogeneous initial conditions

Firstly, the basic model order reduction approach is introduced for the DC microgrid without soft-starting operation in this subsection. Consider the DC microgird (20)-(21) with homogeneous initial conditions:

$$\dot{x}(t) = Ax(t) + Bu(t) \qquad x(0) = 0 \tag{20}$$
$$y(t) = Cx(t) \tag{21}$$

Since the DC microgrid (14)-(15) is stable and in that case, the Lyapunov (22) and (23) have a unique positive semi-definite solution [16]. Thus, the reachability Gramian P and the observability Gramian Q of the DC microgrid are the unique positive-definite ways to the Lyapunov functions, which are shown in (22)-(23). Meanwhile, it is convenient for scholars to obtain P and Q through Matlab.

$$AP + PA^T + BB^T = 0 \tag{22}$$
$$A^TQ + QA + C^TC = 0 \tag{23}$$

The process of the balanced truncation approach is shown as follows: Firstly, define that U and L represent Cholesky factors of P and Q, respectively, *e.g.*, $P = UU^T$ and $Q = LL^T$. Secondly, compute the singular values decomposition (SVD) of $U^TL = G\sum H$ where $\sum = diag(\lambda_1, \lambda_2, ..., \lambda_n)$. The values $\{\lambda_i\}_1^n$ represent the Hankel singular values regarding the DC microgrid (20)-(21). There is no doubt that only one part of the SVD with the large characteristic roots, which are beyond the preset threshold value, should be provided with their associated left/right singular vectors. Thirdly, for one preset reduction order r, Let's

$$V_r = UG_r\Sigma_r^{-0.5} \tag{24}$$
$$W_r = LH_r\Sigma_r^{-0.5} \tag{25}$$

where G_r and H_r represent the leading r columns of G and H, respectively. $\Sigma_r = diag(\lambda_1, \lambda_2, ..., \lambda_r)$, $\lambda_r > \lambda_{r+1}$. The mismatch value between original system and reduced-order system is embedded into order reduction process, which determines the order of the reduced-order system through λ_r and λ_{r+1}. Once the mismatch value is set through power engineers, the order of the system will be determined [3]-[4]. Finally, the state matrix, input matrix and output matrix of the order-r reduced model for the DC microgrid are obtained through balanced truncation approach, which are shown as follows:

$$A_r = W_r^TAV_r \tag{26}$$
$$B_r = W_r^TB \tag{27}$$
$$C_r = CV_r \tag{28}$$

Based on this, the order-r reduced state-space model of the DC microgrid is shown as follows:

$$\dot{x}_r(t) = A_rx_r(t) + B_ru_r(t) \qquad x_r(0) = 0 \tag{29}$$
$$y_r(t) = C_rx_r(t) \tag{30}$$

Remark 3: There is no doubt that the original system inherent characteristics can be reserved. Therein, the DC microgrid is asymptotically stable. Furthermore, the input-output maps error between the original system and reduced-order system satisfies equation (31) [16].

$$\|y(t) - y_r(t)\|_{L_2} \le \left(2\sum_{i=r+1}^{n}\lambda_i\right)\|u(t)\|_{L_2} \tag{31}$$

where $\|X\|_{L_2} \triangleq \left(\int_0^\infty X(t)^TX(t)dt\right)^{0.5}$ represents the norm in the function space L_2^n of square Lebesgue integrable functions $X : [0, \infty) \to R^n$. Because the Hankel singular values are computed consecutively, the number of r is chosen based on the preset error estimation.

B. Model order reduction approach with inhomogeneous initial conditions

In practice, it is impossible that each converter is started without consideration of the soft-starting operation. Based on this, the reduced-order aggregate model based on balanced truncation approach for DC microgrids with inhomogeneous initial conditions is proposed to provide preprocessing for the real-time simulation in this subsection. The output variable $y(t)$ of the DC microgrid (14)-(15) can be rewritten through utilizing the Duhamel formula, which is shown as follows:

$$y(t) = Ce^{At}x_0 + \int_0^t Ce^{A(t-\tau)}Bu(\tau)\,d\tau \tag{32}$$

Define

$$y_{x_0\to y}(t) = Ce^{At}x_0 \quad (33)$$

$$y_{u\to y}(t) = \int_0^t Ce^{A(t-\tau)}Bu(\tau)\,d\tau \quad (34)$$

where e^{At} represents the matrix exponential. For (33), $y_{x_0\to y}(t)$ represents the response from the initial condition x_0 with zero input variable to system output variable, *i.e.*, $u(t) = 0$. For (34), $y_{u\to y}(t)$ represents the response from the input variable $u(t)$ with homogeneous initial conditions to system output variable, *i.e.*, $x_0 = 0$. As a result, since (32) can be linearized into (33) and (34), which satisfies the linearity of the underlying dynamics, the output variable $y(t)$ is the superposition of $y_{x_0\to y}(t)$ and $y_{u\to y}(t)$, *i.e.*, $y(t) = y_{x_0\to y}(t) + y_{u\to y}(t)$. In order to derive the proposed model order reduction approach in detail, the initial value x_0 is rewritten as follows:

$$x_0 = A_0\xi_0 \quad (35)$$

For some $\xi_0 \in R^{n_0}$, in which the columns of A_0 form the basis for subspace of the related initial condition. Therein, the detailed solving process of A_0 is provided in Section 2 regarding the literature [3]. Based on this, the $y_{x_0\to y}(t)$ can be rewritten, which is shown as follows:

$$y_{x_0\to y}(t) = Ce^{At}A_0\xi_0 \quad (36)$$

To this end, the $y_{x_0\to y}(t)$ can be regarded as the response of one dynamical system, which is shown in (37)-(38).

$$\dot{w}(t) = Aw(t) + A_0v(t), \qquad w(0) = 0 \quad (37)$$

$$y_{x_0\to y}(t) = Cw(t) \quad (38)$$

where $v(t) = \xi_0\delta(t)$, and $\delta(t)$ represents the Dirac delta distribution. Based on this, the parameter approximation problem for $y_{x_0\to y}(t)$ (the response to an initial condition with unforced component) can be transformed into one model order reduction problem for one dynamical system with homogeneous initial conditions.

Therefore, the proposed reduced-order aggregate model based on balanced truncation approach can be obtained through paralleled unforced component with nontrivial initial conditions and forced component with null initial conditions. Firstly, the balanced truncation approach, which is introduced in Section III.A, is applied to the following dynamical system.

$$\dot{x}(t) = Ax(t) + Bu(t), \qquad x(0) = 0 \quad (39)$$

$$y_{u\to y}(t) = Cx(t) \quad (40)$$

According to balanced truncation approach, the corresponding reduced-order model for forced component with null initial conditions is provided as follows:

$$\dot{x}_{r1}(t) = A_{r1}x_{r1}(t) + B_{r1}u(t), \qquad x_{r1}(0) = 0 \quad (41)$$

$$y_{r1}(t) = C_{r1}x_{r1}(t) \quad (42)$$

where $r1$ represents the dimension of the proposed reduced-order model for forced component. Similarly, the balanced truncation approach can also be applied to the dynamical system (37)-(38). To this end, the corresponding reduced-order model for unforced component with nontrivial initial conditions is provided through balanced truncation approach, which is shown as follows:

$$\dot{x}_{r2}(t) = A_{r2}x_{r2}(t) + B_{r2}u(t), \qquad x_{r2}(0) = 0 \quad (43)$$

$$y_{r2}(t) = C_{r2}x_{r2}(t) \quad (44)$$

where $r2$ represents the dimension of the proposed reduced-order model for unforced component. In the end, in order to approximate the total output variable $y(t)$ in (14)-(15) with $x_0 = A_0\xi_0$, the superposition of the output variable $y_{u\to y}(t)$ in (33) and $y_{x_0\to y}(t)$ in (34) with $v(t) = \xi_0\delta(t)$ is reduced in parallel. With these efforts, the final approximation of the output variable $y_r(t)$ can be provided as follows:

$$y_r(t) = y_{r1} + y_{r2} \quad (45)$$

Under zero initial conditions, the unforced component will be ignored, and the proposed model order reduction approach will be the same as the traditional model order reduction approach [16]. The system with zero initial conditions is one particular case for this paper. This scenario illustrates that the proposed approach in this paper can be suitable for different cases, which is an important advantage. Due to the soft-starting operation for DC microgrids, there is no doubt that the power system initial values are not always zero [5]. If initial values are wrongly ignored, the input-output maps error will be large, which is difficult for real-time simulators of DC microgrids to adopt this reduced order model. For this special case, an improved model order reduction approach based on the literature [4] is first applied in DC microgrids, which is an important innovation. Meanwhile, the error bound theorem is also first applied in power system. Before real-time simulation, the errors between the output variables of the full order model and the output variables of the reduced order model can be provided through error bound theorem. If this error can be accepted through DC microgrid designers, the DC microgrid system designer can use the reduced-order model to design the secondary controller and research the dynamic characteristics. Under this case, the full order model can be ignored and real-time simulation process can be cancelled. To this end, it is very significant to apply to DC microgrids rather than stay at the theoretical level. Furthermore, for this special system, a DC microgrid, the system model should be built in advance. Based on this model, the subsequent model order reduction approach can be studied. That is exactly what this paper does. In order to reduce computational burden, the process of the model order reduction with inhomogeneous initial conditions can be divided into two phases, *i.e.*, off-line phase and on-line phase. Therein, the foresaid two parts in (45) can be obtained in parallel through an off-line phase before utilizing the reduced order model for real-time simulation. The detailed process can be shown in **Algorithm 1** and **Algorithm 2**.

Remark 4: In order to decrease the computational burden, the model order reduction process of balanced truncation can be replaced by the other previous model order reduction approaches, such as Iterative Rational Krylov Algorithm (IRKA), Sparse LRCF-ADI (SLRCF-ADI) and so on

Algorithm 1 Off-line Phase: Construct the basic reduced-order aggregate model

Input: The dynamical system matrices A, B, C, and the initial condition matrix A_0.
Output: Reduced mappings for $F_{u\to y}$ and $F_{x_0\to y}$.

1: Approximating $F_{u\to y}$: Apply model order reduction approach to $F_{u\to y}$: $\dot{x}(t) = Ax(t) + Bu(t), \quad x(0) = 0, \quad y_u(t) = Cx(t)$;
2: Obtain the reduced-order model $F_{ru\to y}$ for forced component, *i.e.*, $F_{ru\to y}$: $\dot{x}_{r1}(t) = A_{r1}x_{r1}(t) + B_{r1}u(t), \quad x_{r1}(0) = 0, \quad y_{r1}(t) = C_{r1}x_{r1}(t)$;
3: Approximating $F_{x_0\to y}$: Apply model order reduction approach to $F_{x_0\to y}$: $\dot{w}(t) = Aw(t) + A_0v(t), \quad w(0) = 0, \quad y_{x_0}(t) = Cw(t)$;
4: Obtain the reduced-order model $F_{rx_0\to y}$ for unforced component, *i.e.*, $F_{x_0\to y}$: $\dot{x}_{r2}(t) = A_{r2}x_{r2}(t) + B_{r2}u(t), \quad x_{r2}(0) = 0, \quad y_{r2}(t) = C_{r2}x_{r2}(t)$.

Algorithm 2 On-line Phase: Construct the reduced-order aggregate model for real-time simulation

Input: The initial condition x_0 and the forcing term $u(t)$.
Output: The approximate reduced-order output variable $y_r(t)$.

1: Compute ξ_0 such that $x_0 = A_0\xi_0$;
2: Simulate $F_{ru\to y}$ with input variable $u(t)$ and homogeneous initial condition to provide the output variable $y_{r1}(t)$;
3: Simulate $F_{rx_0\to y}$ with null input variable $u(t) = 0$ and inhomogeneous initial condition ξ_0 to provide the output variable $y_{r2}(t)$;
4: Compute approximate output variable: $y_r(t) = y_{r1}(t) + y_{r2}(t)$.

[16]. Meanwhile, the other model order reduction process is not changed, which is an important advantage for the proposed model order reduction approach. Furthermore, the MATLAB code for model order reduction approach with homogeneous initial conditions can be found at the website: https://sites.google.com/site/rommes/software, which is provided in the literature [16]. Furthermore, the load practical DC microgrid usually changes over time, which results in the parameter perturbations. Fortunately, this issue has been solve in the previous literature [21], where the parameter perturbation term can be reserved in the reduced-order process. Based on this, if the model order reduction process of balanced truncation in this paper is replaced through the parameter preserving model order reduction approach in the literatures [21], the parameter perturbation problem can be well solved. Meanwhile, one real DC microgrid has various DGs, such as solar generator, wind generator and so on. Fortunately, the researches regarding certain generator have been widely proposed in the previous literatures, such as wind generator, Li-Ion and so on. For each specific DG, the state-space function should be rebuilt to reflect the different dynamic characteristics. This paper pays more attention on general system, and each DG is regarded as an ideal DC voltage source. This operation has been widely applied in the previous literatures [21]-[26]. Of course, once the state-space function is provided, the proposed model order reduction approach in this paper can also be applied to power system consisting of one or more DG.

Remark 5: If the initial condition contributes to a large amount of energy in the augmented system, the reduced-order model with a higher order will be required. Meanwhile, this will also increase the computational and control complexity while operating the controller in real time. In this paper, the original full-order state-space function is divided into two components, i.e., the unforced component with nontrivial initial conditions and forced component with null initial conditions. Therein, the unforced component represents the impact of the initial conditions. Under this initial condition, the order of the reduced-order model regarding unforced component will be high. There is an important trade-off between model accuracy and computational complexity. However, if you want to obtain one lower order model, whose order is the same as the reduced order model based on the conventional approach, the output variable error between full order model and reduced order model for unforced component can be chosen as one large value. Under this case, the order of the reduced order model based on the proposed approach in this paper can be the same as that based on the conventional approach. Meanwhile, the model accuracy is still improved through the proposed model reduction approach. Furthermore, this paper focuses more on the system modeling and its model order reduction. There is no doubt that the relative controller based on the proposed reduced-order model in this paper can be designed. Therein, the control performance is better if it is based on one more accurate model. To my best knowledge, the hierarchical control has been proposed to solve relative problem, such as current sharing and so on. Therein, the distributed secondary control strategy proposed in the literature [11] is proposed, which is based on multi-agent consistency control.

IV. Approximated Error Bound of the Proposed Reduced-Order Aggregate Model

It is important for real-time simulation researchers to obtain the approximated error bound between the original system and reduced-order system in advance. To this end, this section provides an error bound for approximation error $\|y(t) - y_r(t)\|_{L_2}$, which is obtained through the proposed model order reduction approach.

Firstly, for the unforced component, let (37)-(38) be one full balanced realization. For certain preset reduced order r_2, partition A, A_0 and C conformingly as

$$A=\left[\begin{array}{cc} A_{11} & A_{12} \\ A_{21} & A_{22} \end{array}\right], A_0=\left[\begin{array}{c} A_{01} \\ A_{02} \end{array}\right], C=\left[\begin{array}{cc} C_1 & C_2 \end{array}\right] \quad (46)$$

where $A_{11} \in R^{r_2 \times r_2}$, $A_{01} \in R^{r_2 \times N}$, and $C_1 \in R^{N \times r_2}$. Furthermore, define that W is a solution of the Sylvester function

$$A^T W + W A_{11} + C^T C_1 = 0 \quad (47)$$

Define that $\partial = diag\left(\delta_1, \delta_2, ..., \delta_{3N}\right)$ is the diagonal matrix of Hankel singular values of (37)-(38). Based on this, partition W and ∂ can be rewritten as follows:

$$W=\left[\begin{array}{c} W_1 \\ W_2 \end{array}\right], \partial=\left[\begin{array}{cc} \partial_1 & 0 \\ 0 & \partial_2 \end{array}\right] \quad (48)$$

where $W_1, \partial_1 \in R^{r_2 \times r_2}$. Define

$$F_{x_0}(t) = Ce^{At}A_0 \quad (49)$$

$$F_{r2x_0}(t) = C_{r2}e^{A_{r2}t}A_{r0} \quad (50)$$

where $F_{x_0}(t)$ represents the impulse response of the full-model in (37)-(38), and $F_{r2x_0}(t)$ represents the impulse response of the reduced-order model in (43)-(44). As a result, the approximation error is shown as follows [4]

$$\left\|F_{x_0}(t) - F_{r2x_0}(t)\right\|_{L_2}^2 \leq trace\left[\wp_1\partial_2 + \wp_2\partial_2\right] \quad (51)$$

where $\wp_1 = A_{02}A_{02}^T$, $\wp_2 = 2W_2A_{12}$ and $\wp = \wp_1 + \wp_2$. Therein, the former term in the upper bound (51), *e.g.*, $trace[\wp_1\partial_2]$ depends on the neglected Hankel singular values ∂_2, and the latter term in the upper bound (51), *e.g.*, $trace[\wp_2\partial_2]$ depends quadratically on ∂_2. Through the foresaid theoretical accumulation, the upper bound of the approximation error for the proposed model order reduction approach is provided as follows:

Theorem 1: Assume that $y(t)$ is the output variable of the full-order model in (15) with inhomogeneous initial condition x_0. Meanwhile, $y_r(t)$ is the reduced-order output variable, which is obtained through **Algorithm 1** and **Algorithm 2**. Based on this, for abnormal input variable $u(t) \in L_2^N$, the output variable error $y(t) - y_r(t)$ is bounded through

$$\left\|y(t) - y_r(t)\right\|_{L_2} \leq \left(2\sum_{i=r_1+1}^{3N}\lambda_i\right)\left\|u(t)\right\|_{L_2} + \sqrt{trace\left[\wp\partial_2\right]}\left\|\xi_0\right\|_{L_2} \quad (52)$$

where λ_i $(i = r_1+1, r_1+2, ..., 3N)$ represents the truncated Hankel singular values in (41)-(42). δ_i $(i = r_2+1, r_2+2, ..., 3N)$ represents the truncated Hankel singular values in (43)-(44).

Proof: Recall from (32) that $y(t) = y_1(t) + y_2(t)$ and from (45) that $y_r(t) = y_{r1} + y_{r2}$. Thus,

$$\left\|y(t) - y_r(t)\right\|_{L_2} \leq \left\|y_1(t) - y_{r1}(t)\right\|_{L_2} + \left\|y_2(t) - y_{r2}(t)\right\|_{L_2} \quad (53)$$

The former term of the upper bound in (53) is provided through utilizing the balanced truncation upper bound in (31). Since $y_1(t)$ is the output variable of the reduced-order model approximation to (39)-(40) provided through balanced truncation approach, and therefore

$$\left\|y_1(t) - y_{r1}(t)\right\|_{L_2} \leq \left(2\sum_{i=r_1+1}^{3N}\lambda_i\right)\left\|u(t)\right\|_{L_2} \quad (54)$$

For latter term of the upper bound in (53), *i.e.*, $\left\|y_2(t) - y_{r2}(t)\right\|_{L_2}$, the definitions of $y_2(t)$ in (40) and $y_{r2}(t)$ in (44) are applied, and therefore

$$\left\|y_2(t) - y_{r2}(t)\right\|_{L_2} \leq \sqrt{trace\left[\wp\partial_2\right]}\left\|\xi_0\right\|_{L_2} \quad (55)$$

Therefore, the proof is finished.

Remark 6: The error bound in (52) for output variable response illustrates the value of proposed model order reduction for two mappings $F_{ru\to y}$ and $F_{rx_0\to y}$ independently. First of all, scholars can choose the reduced dimensions r_1 and r_2 independent of each other, which is based on preset error thresholds. Then, with independent reduction of $F_{u\to y}$ and $F_{x_0\to y}$, the scaling of input variable maps and inhomogeneous initial conditions are not coupled. To this end, the resulting reduced-order models is scale-independent, which is one of the main advantages of the proposed model order reduction approach. Furthermore, the prior knowledge and theoretical basis could be provided for DC microgrid designers through this theorem. Before real-time simulation, the errors between the output variables of the full order model and the output variables of the reduced order model can be provided through error bound theorem. If this error can be accepted through DC microgrid designers, the DC microgrid designer can use the reduced-order model to design the secondary controller and research the dynamic characteristics. Under this case, the full order model can be ignored and real-time simulation process can also be canceled.

V. Simulation and Experiment

In this section, the proposed model order reduction approach is verified through DC microgrid built in this paper. In order to reveal the result performance based on the proposed model order reduction approach, L_∞ *error* (L_∞ *error*=$\left\|y(t) - y_r(t)\right\|_{L_\infty}$) and L_2 *error* (L_2 *error*=$\left\|y(t) - y_r(t)\right\|_{L_2}$) are provided, which are two important indexes for evaluating the performance of the model order reduction approach [30]. In order to simplify the system complexity, assume that there are four different parameters of agents in this DC microgrid, *i.e.*, $Agent_I$, $Agent_{II}$, $Agent_{III}$ and $Agent_{IV}$. Meanwhile, the rated dc voltage is $50V$, and the ratio of rated capacities regarding each DG in different agent is set as $DG_I : DG_{II} : DG_{III} : DG_{IV} = 1 : 2 : 3 : 4$. The converter rating values of four DGs are chosen as 2kW, 4kW, 6kW and 8kW, respectively. The detailed parameters of each DG are shown in Table I.

A. Model Accuracy Verification

In order to visually verify the model accuracy, the number of the agents in DC microgrid is chosen as four, *i.e.*, $Agent_I$, $Agent_{II}$, $Agent_{III}$ and $Agent_{IV}$. Meanwhile, the line resistance R_{ij} between the i^{th} agent and the j^{th} agent are shown

TABLE I: The DC microgrid simulation parameters regarding four agents

Detailed parameters of the $Agent_I$		
Parameter Meaning	Symbol	Value
$V-I$ droop coefficient	m_I	0.01
Resistor for RLC Filter	R_{fI}	0.1Ω
Inductor for RLC Filter	L_{fI}	$0.8mH$
Capacitor for RLC Filter	C_{fI}	$2.2mF$
Common resistor load	R_{LI}	2Ω
First term in PnP controller	$n_{I,1}$	-5
Second term in PnP controller	$n_{I,2}$	-0.1
Third term in PnP controller	$n_{I,3}$	25
Detailed parameters of the $Agent_{II}$		
Parameter Meaning	Symbol	Value
$V-I$ droop coefficient	m_{II}	0.0075
Resistor for RLC Filter	R_{fII}	0.05Ω
Inductor for RLC Filter	L_{fII}	$0.4mH$
Capacitor for RLC Filter	C_{fII}	$1.1mF$
Common resistor load	R_{LII}	4Ω
First term in PnP controller	$n_{II,1}$	-5
Second term in PnP controller	$n_{II,2}$	-0.1
Third term in PnP controller	$n_{II,3}$	25
Detailed parameters of the $Agent_{III}$		
Parameter Meaning	Symbol	Value
$V-I$ droop coefficient	m_{III}	0.005
Resistor for RLC Filter	R_{fIII}	0.025Ω
Inductor for RLC Filter	L_{fIII}	$0.2mH$
Capacitor for RLC Filter	C_{fIII}	$0.55mF$
Common resistor load	R_{LIII}	10Ω
First term in PnP controller	$n_{III,1}$	-5
Second term in PnP controller	$n_{III,2}$	-0.1
Third term in PnP controller	$n_{III,3}$	25
Detailed parameters of the $Agent_{IV}$		
Parameter Meaning	Symbol	Value
$V-I$ droop coefficient	m_{IV}	0.0025
Resistor for RLC Filter	R_{fIV}	0.01Ω
Inductor for RLC Filter	L_{fIV}	$0.08mH$
Capacitor for RLC Filter	C_{fIV}	$0.22mF$
Common resistor load	R_{LIV}	4Ω
First term in PnP controller	$n_{IV,1}$	-5
Second term in PnP controller	$n_{IV,2}$	-0.1
Third term in PnP controller	$n_{IV,3}$	25

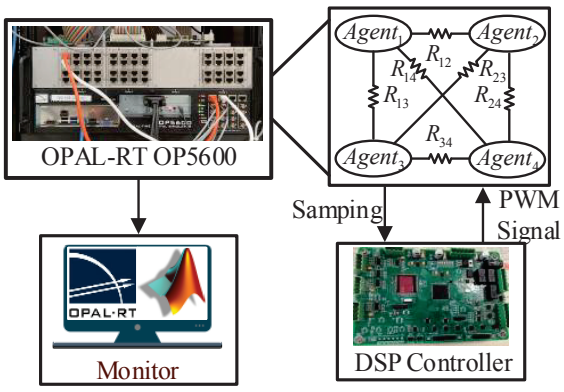

Fig. 3: The CHIL experiment test system.

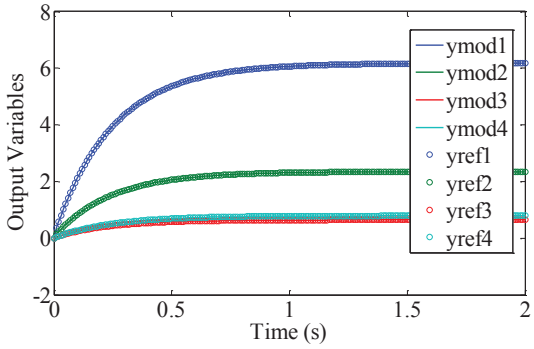

Fig. 4: The output variables between practical experimental system in the CHIL experiment setup and full-order state-space function in the simulation setup.

as follows: $R_{12}=R_{21}=2.3\Omega$, $R_{13}=R_{31}=2.1\Omega$, $R_{14}=R_{41}=2.7\Omega$, $R_{23}=R_{32}=2.9\Omega$, $R_{24}=R_{42}=1.5\Omega$ and $R_{34}=R_{43}=2.5\Omega$. In order to better reflect the real power system, the four agents are different in hardware-in-the-loop (CHIL) experiment test system. From Table I, there are three different points, i.e., rated power difference, line impedance difference and load difference. Firstly, the droop coefficient of each distributed generator is designed in inverse proportion to its rated current, i.e., $m_1I_1=m_2I_2=...=m_NI_N$. To this end, each agent has different rated power or current. Secondly, the RLC filter of each agent is different, which illustrates that the line impedance of each agent is different. Thirdly, the load of each agent is different in the CHIL experiment test system. Based on this, the state matrix A_{ii} of each agent is different, which results in that the system model belongs to linear heterogeneous multiagent systems. The test system is executed in the CHIL experiment test system, which is shown in Fig. 3. The detailed illustration regarding the CHIL experiment test system can be found in our previous literatures [8], [31]. Under these parameters, the dimension of the original system (14)-(15) is twelve, *i.e.*, $A_{12\times12}$, $B_{12\times4}$ and $C_{4\times12}$. Furthermore, the detailed form is shown in the appendix. Through observing the relative matrices, it is obvious that only the A_{ij} and A_{ii} regarding the increased/decreased agent are provided in full-order system. To this end, it is convenient for scholars to build complex system modeling with switched topology or "plug and play" feature. Moreover, the output variables between practical experimental system and full-order state-space function are shown in Fig. 4. Therein, y_{refi} and $y_{\bmod i}$ represents the output variables for the i^{th} agent based on practical experimental system and full-order state-space function, respectively. Moreover, the reference system is the CHIL experiment test system. Therein, the model accuracy can be verified through comparing the output variables of the CHIL experiment test system with the output variables of the full-order state-space function in the simulation setup. To this end, the output variable curve of the full-order state-space function can give adequate overall fits with the practical experimental system, which is shown in Fig. 4. Thus, the model accuracy can be ensured through the foresaid experimental results.

B. Model Order Reduction Approach Verification

In order to visually verify the effectiveness of the proposed model order reduction approach, the number of the agents in DC microgrid is also chosen as four. The detailed simulation parameters are the same as those in the foresaid subsection. Assume that the initial condition of the first agent is inhomogeneous, *i.e.*, $x_1=(V_1,I_{f1},\bar{z}_1)^T=(45,6,0)$, and the other three agents are homogeneous, *i.e.*, $x_2=x_3=$

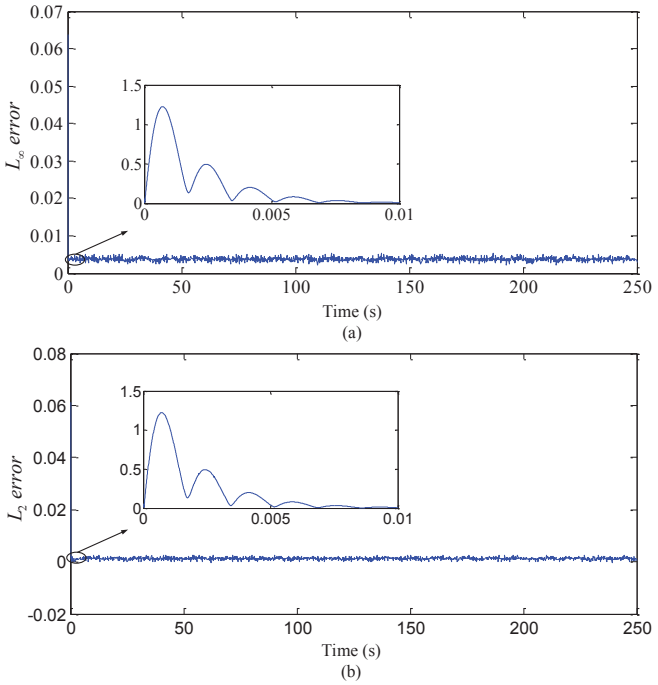

Fig. 5: The errors based on the literatures [16] and [21] between the output of the full order model and the output of the reduced order model: (a) L_∞ $error$=$\|y(t)-y_r(t)\|_{L_\infty}$; (b) L_2 $error$ (L_2 $error$=$\|y(t)-y_r(t)\|_{L_2}$.

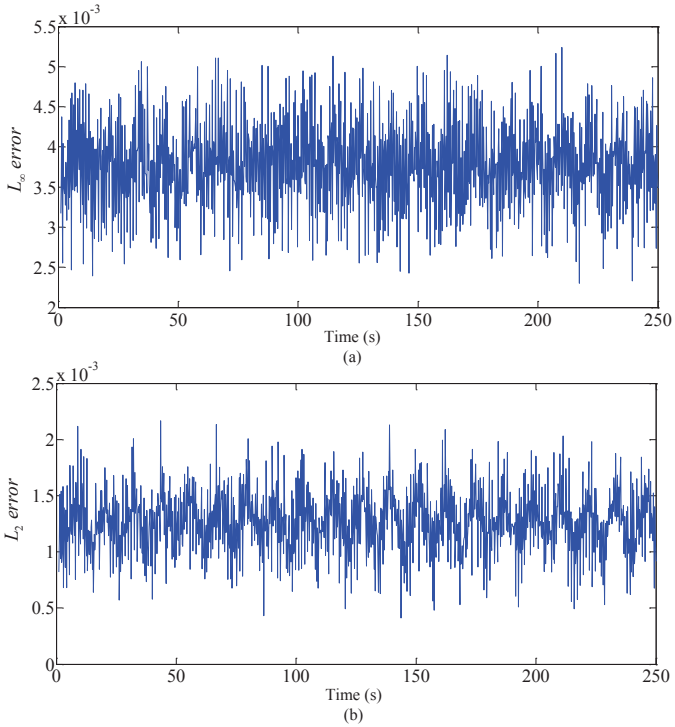

Fig. 6: The errors based on the proposed approach between the output of the full order model and the output of the reduced order model: (a) L_∞ $error$=$\|y(t)-y_r(t)\|_{L_\infty}$; (b) L_2 $error$ (L_2 $error$=$\|y(t)-y_r(t)\|_{L_2}$.

$x_4 = (0,0,0)^T$. To this end, the matrix A_0 can be the 12-dimension unit matrix, and the reduced order numbers, *i.e.*, r_1 and r_2, can be chosen as $r_1 = 4$ and $r_2 = 8$, respectively. There is no doubt that the resulting reduced-order models (r_1 and r_2) can be scale independent. In this subsection, the reference system is the original full-order state-space function shown in (14)-(15), and output error in this paper represents the error between the output variables of the original full-order state-space function and the output variables of the reduced order state-space function. The errors based on the literatures [16] and [21] between the output variables of the full order model and the output variables of the reduced order model are provided in Fig. 5. There is no doubt that these errors cannot be accepted for real-time simulation engineers in the initial stage. Meanwhile, the errors based on proposed approach between the output variables of the full order model and the output variables of the reduced order model are provided in Fig. 6. Obviously, the output variable curve of the reduced-order model better gives adequate overall fits with the full-order model at all times. Finally, the L_∞ $error$ and L_2 $error$ based on the proposed model order reduction approach are shown as follows: L_∞ $error = 3.7816 \times 10^{-3}$ and L_2 $error = 1.2687 \times 10^{-3}$. The result regarding the input-output maps error is acceptable for real-time simulation scholars.

In order to illustrate that the proposed model order reduction approach is suitable for the complex DC microgrid with numerous agents/DGs, three DC microgrids consisting of different agents are provided to verify the effectiveness of the proposed model order reduction approach. Therein, the types of agents are sorted as follows: ($Agent_I, Agent_{II}, Agent_{III}, Agent_{IV}, Agent_I, ...$). Meanwhile, the initial condition regarding the first quartile of agents is inhomogeneous, which is shown as follows:

$$x_0 = (\underbrace{45,6,0,...,45,6,0}_{3N/4},\underbrace{0,0,0,...,0,0,0}_{9N/4}) \quad (56)$$

Based on this, L_∞ $error$ and L_2 $error$ under the different number of agents are shown in Table II. The relative results regarding the input-output maps error are also acceptable for real-time simulation scholars. Therefore, the effectiveness of the proposed model order reduction approach can be verified.

TABLE II: The DC microgrid simulation parameters regarding four agents

Number	L_∞ $error$	L_∞ $error$
20	4.3926×10^{-3}	3.6214×10^{-3}
60	5.3128×10^{-3}	3.9867×10^{-3}
100	6.2145×10^{-3}	4.3268×10^{-3}

C. Previous numerical model verification

In order to verify the high performance of the proposed model order reduction approach, which is compared with the the pure theoretical literature [3], the previous numerical model found on Section 6.1 of the literature [30] is provided.

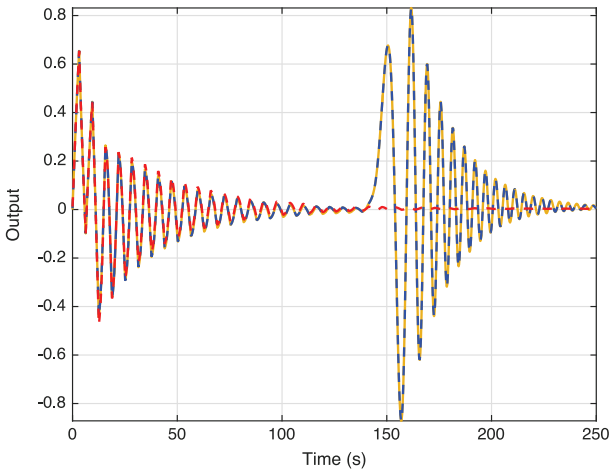

Fig. 7: The performance comparison with the pure theoretical literature [3].

Therein, the numbers of state variable, input variable and output variable are individually set as three hundred, ten and one. Meanwhile, the input variables are the external forcing on the top ten masses and the output variable is the momentum of the first mass. Furthermore, one one-dimensional subspace for the inhomogeneous initial condition $x_0 = 1$ is chosen. To this end, the matrix A_0 can be the $n-$dimension unit matrix. The truncation tolerance of 0.01 is determined to produce reduced order, which is based on the decay rate. Based on this, the reduced order numbers, *i.e.*, r_1 and r_2, can be chosen as $r_1 = 16$ and $r_2 = 98$, respectively. There is no doubt that the resulting reduced-order models (r_1 and r_2) can be scale independent. In order to illustrate the high performance, the output variable curves among the full-order model (yellow curve), the reduced-order model based on the proposed approach in [3] (red curve) and the reduced-order model based on the proposed approach in this paper (blue curve) are provided in Fig. 7. Therein, the output variable curve of the reduced-order model better gives adequate overall fits with the full-order model. To sum up, the effectiveness of the proposed model order reduction approach can be verified.

VI. Conclusion

With the rapid development regarding the high penetration of distributed renewable sources, the model order reduction approach has been indispensable for the real-time simulation. Although the traditional model order reduction approaches have been widely studied, the initial values requirement has been always ignored or it has been avoided through making the restrictive assumption that the initial values are zero. Apparently, it is difficult for real-time simulation scholars to accept this result due to soft-starting operation. To this end, this paper has proposed a reduced-order aggregate model based on balanced truncation approach to provide the preprocessing approach for the real-time simulation of large-scale converters with inhomogeneous initial conditions in DC microgrid. Compared with the existing literatures, three advantages have been found in this paper as follows: (*i*) The standard linear time-invariant model with inhomogeneous initial conditions has been built through non-leader multiagents concept. With this effect, it has been convenient for scholars to build complex system modeling with switched topology or "plug and play" feature. Meanwhile, this modeling concept can be applied to relative fields, such as AC microgrid, AC/DC microgrid, smart grid and so on; (*ii*) For the foresaid system, the reduced-order aggregate model based on balanced truncation approach has been presented to provide preprocessing for the real-time simulation. Based on this, the errors between the output variables of the full order model and the output variables of the reduced order model have been reduced; (*iii*) The approximated error estimate of the reduced-order aggregate model regarding large-scale converters has been provided through using the mathematical theorem 1. To this end, the prior knowledge and theoretical basis could be provided for DC microgrid designers. Finally, the simulation results have been provided to verify the performance of the proposed model order reduction approach.

Appendix
Detailed sub-matrices for the original system with four DGs

$$A_{11} = \begin{bmatrix} -227 & 455 & 0 \\ -7500 & -250 & 31250 \\ 1 & 0 & 0 \end{bmatrix}, \quad A_{12} = \begin{bmatrix} -197 & 0 & 0 \\ 0 & 0 & 0 \\ 0 & 0 & 0 \end{bmatrix}, \quad A_{13} = \begin{bmatrix} -216 & 0 & 0 \\ 0 & 0 & 0 \\ 0 & 0 & 0 \end{bmatrix},$$
$$A_{14} = \begin{bmatrix} -168 & 0 & 0 \\ 0 & 0 & 0 \\ 0 & 0 & 0 \end{bmatrix}, A_{21} = \begin{bmatrix} -395 & 0 & 0 \\ 0 & 0 & 0 \\ 0 & 0 & 0 \end{bmatrix} A_{22} = \begin{bmatrix} -227 & 909 & 0 \\ -1500 & -375 & 62500 \\ 1 & 0 & 0 \end{bmatrix}, \quad A_{23} = \begin{bmatrix} -313 & 0 & 0 \\ 0 & 0 & 0 \\ 0 & 0 & 0 \end{bmatrix},$$
$$A_{24} = \begin{bmatrix} -606 & 0 & 0 \\ 0 & 0 & 0 \\ 0 & 0 & 0 \end{bmatrix}, A_{31} = \begin{bmatrix} -865 & 0 & 0 \\ 0 & 0 & 0 \\ 0 & 0 & 0 \end{bmatrix}, A_{32} = \begin{bmatrix} -865 & 0 & 0 \\ 0 & 0 & 0 \\ 0 & 0 & 0 \end{bmatrix}, A_{33} = \begin{bmatrix} -180 & 1820 & 0 \\ -30000 & -630 & 125000 \\ 0 & 0 & 0 \end{bmatrix},$$
$$A_{34} = \begin{bmatrix} -727 & 0 & 0 \\ 0 & 0 & 0 \\ 0 & 0 & 0 \end{bmatrix}, A_{41} = \begin{bmatrix} -1683.5 & 0 & 0 \\ 0 & 0 & 0 \\ 0 & 0 & 0 \end{bmatrix},$$
$$A_{42} = \begin{bmatrix} -3030 & 0 & 0 \\ 0 & 0 & 0 \\ 0 & 0 & 0 \end{bmatrix}, A_{43} = \begin{bmatrix} -1818 & 0 & 0 \\ 0 & 0 & 0 \\ 0 & 0 & 0 \end{bmatrix},$$
$$A_{44} = \begin{bmatrix} -1140 & 4550 & 0 \\ -75000 & -1380 & 312500 \\ 0 & 0 & 0 \end{bmatrix}, B_{11} = B_{22} = B_{33} = B_{44} = \begin{bmatrix} -5 & -0.1 & 25 \end{bmatrix}^T, C_{11} = \begin{bmatrix} 0 & 0.01 & 0 \end{bmatrix},$$
$$C_{22} = \begin{bmatrix} 0 & 0.0075 & 0 \end{bmatrix}, C_{33} = \begin{bmatrix} 0 & 0.005 & 0 \end{bmatrix},$$
$$C_{44} = \begin{bmatrix} 0 & 0.0025 & 0 \end{bmatrix}.$$

Acknowledgement

Authors would like to thank F. Freitas, J. Rommes, and N. Martins to use their MATLAB code regarding model order reduction approach with homogeneous initial conditions.

REFERENCES

[1] J. Ma, Y. Zhang, Y. Shen, P. Cheng and A. G. Phadke, "Equipment-level locating of Low Frequency Oscillating Source in Power System with DFIG Integration Based on Dynamic Energy Flow," *IEEE Trans. Power Syst.*, vol. 35, no. 5, pp. 3433-3447, Sept. 2020.

[2] V. Purba, B. B. Johnson, M. Rodriguez, S. Jafarpour, F. Bullo and S. V. Dhople, "Reduced-order Aggregate Model for Parallel-connected Single-phase Inverters," *IEEE Trans. Energy Convers.*, vol. 34, no. 2, pp. 824-837, June 2019.

[3] Heinkenschloss M, Reis T, Antoulas A C, "Balanced truncation model reduction for systems with inhomogeneous initial conditions," *Automatica*, vol. 47, no. 3, pp. 559-564, Jan 2011.

[4] Beattie C, Gugercin S, Mehrmann V, "Model Reduction for Systems with Inhomogeneous Initial Conditions," *Syst. Control Lett*, vol. 99, pp. 99-106, Jan 2017.

[5] S. Pugliese, G. Buticchi, R. A. Mastromauro, M. Andresen, M. Liserre and S. Stasi, "Soft-Start Procedure for a Three-Stage Smart Transformer based on Dual Active Bridge and Cascaded H-Bridge Converters," *IEEE Trans. Power Electron.*, vol. 35, no. 10, pp. 11039-11052, Oct. 2020.

[6] W. Rui, S. Qiuye, M. Dazhong and H. Xuguang, "Line Impedance Cooperative Stability Region Identification Method for Grid-Tied Inverters Under Weak Grids," *IEEE Trans. Smart Grid*, vol. 11, no. 4, pp. 2856-2866, July 2020.

[7] Z. Shuai, Y. Li, W. Wu, C. Tu, A. Luo and Z. J. Shen, "Divided DQ Small-Signal Model: A New Perspective for the Stability Analysis of Three-Phase Grid-Tied Inverters," *IEEE Trans. Ind. Electron.*, vol. 66, no. 8, pp. 6493-6504, Aug. 2019.

[8] W. Rui, S. Qiuye, Z. Pinjia, G. Yonghao, Q. Dehao and W. Peng, "Reduced-Order Transfer Function Model of the Droop-Controlled Inverter via Jordan Continued-Fraction Expansion," *IEEE Trans. Energy Convers.*, vol. 35, no. 3, pp. 1585-1595, Sept. 2020.

[9] E. A. A. Coelho, P. C. Cortizo and P. F. D. Garcia, "Small-signal stability for parallel-connected inverters in stand-alone AC supply systems," *IEEE Trans. Ind. Appl.*, vol. 38, no. 2, pp. 533-542, March-April 2002.

[10] N. Pogaku, M. Prodanovic and T. C. Green, "Modeling, Analysis and Testing of Autonomous Operation of an Inverter-Based Microgrid," *IEEE Trans. Power Electron.*, vol. 22, no. 2, pp. 613-625, March 2007.

[11] J. Zhou, Y. Xu, H. Sun, L. Wang and M. Chow, "Distributed Event-Triggered H_∞ Consensus Based Current Sharing Control of DC Microgrids Considering Uncertainties," *IEEE Trans. Ind. Informa.*, doi: 10.1109/TII.2019.2961151.

[12] F. D. Freitas, N. Martins, S. L. Varricchio, J. Rommes and F. C. Veliz, "Reduced-Order Transfer Matrices From RLC Network Descriptor Models of Electric Power Grids," *IEEE Trans. Power Syst.*, vol. 26, no. 4, pp. 1905-1916, Nov. 2011.

[13] L. Luo and S. V. Dhople, "Spatiotemporal Model Reduction of Inverter-Based Islanded Microgrids," *IEEE Trans. Energy Convers.*, vol. 29, no. 4, pp. 823-832, Dec. 2014.

[14] J. Chow, R. Galarza, P. Accari, and W. Price, "Inertial and slow coherency aggregation algorithms for power system dynamic model reduction," *IEEE Trans. Power Syst.*, vol. 10, no. 2, pp. 680-685, May. 1995.

[15] D. Chaniotis and M. A. Pai, "Model reduction in power systems using Krylov subspace methods," *IEEE Trans. Power Syst.*, vol. 20, no. 2, pp. 888-894, May. 2005.

[16] F. Freitas, J. Rommes, and N. Martins, "Gramian-based reduction method applied to large sparse power system descriptor models," *IEEE Trans. Power Syst.*, vol. 23, no. 3, pp. 1258-1270, Aug. 2008.

[17] H. Li, J. Fang and Y. Tang, "Dynamic Phasor-Based Reduced-Order Models of Wireless Power Transfer Systems," *IEEE Trans. Power Electron.*, vol. 34, no. 11, pp. 11361-11370, Nov. 2019.

[18] D. Osipov and K. Sun, "Adaptive Nonlinear Model Reduction for Fast Power System Simulation," *IEEE Trans. Power Syst.*, vol. 33, no. 6, pp. 6746-6754, Nov. 2018.

[19] G. Fan, X. Li and M. Canova, "A Reduced-Order Electrochemical Model of Li-Ion Batteries for Control and Estimation Applications," *IEEE Trans. Veh. Technol.*, vol. 67, no. 1, pp. 76-91, Jan. 2018.

[20] H. R. Ali, L. P. Kunjumuhammed, B. C. Pal, A. G. Adamczyk and K. Vershinin, "A Trajectory Piecewise-Linear Approach to Nonlinear Model Order Reduction of Wind Farms," *IEEE Trans. Sustain. Energy*, vol. 11, no. 2, pp. 894-905, April 2020.

[21] Y. G. I. Acle, F. D. Freitas, N. Martins and J. Rommes, "Parameter Preserving Model Order Reduction of Large Sparse Small-Signal Electromechanical Stability Power System Models," *IEEE Trans. Power Syst.*, vol. 34, no. 4, pp. 2814-2824, July 2019.

[22] I. P. Nikolakakos, H. H. Zeineldin, M. S. El-Moursi and J. L. Kirtley, "Reduced-Order Model for Inter-Inverter Oscillations in Islanded Droop-Controlled Microgrids," *IEEE Trans. Smart Grid*, vol. 9, no. 5, pp. 4953-4963, Sept. 2018.

[23] M. Su, Z. Liu, Y. Sun, H. Han, X. Hou, "Stability Analysis and Stabilization methods of DC Microgrid with Multiple Parallel-Connected DC-DC Converters loaded by CPLs," *IEEE Trans. Smart Grid*, vol. 9, no.1, pp.132-142, Jan. 2018.

[24] Z. Liu, M. Su, Y. Sun, W. Yuan and H. Han, "Existence and Stability of Equilibrium of DC Microgrid with Constant Power Loads," *IEEE Trans. Power Syst.*, vol. 33, no. 6, pp. 6999-7010, Nov, 2018.

[25] Z. Liu, R. Liu, X. Zhang, M. Su, Y. Sun, H. Han, P. Wang, "Feasible Power-Flow Solution Analysis of DC Microgrids under Droop Control," *IEEE Trans. Smart Grid*, vol. 11, no. 4, pp. 2771-2781, July, 2020.

[26] Anand, Sandeep, Fernandes, B. G. "Reduced-Order Model and Stability Analysis of Low-Voltage DC Microgrid," *IEEE Trans. Ind. Electron.*, vol. 60, no. 11, pp. 5040-5049, Nov. 2013.

[27] Q. Sun, R. Han, H. Zhang, J. Zhou and J. M. Guerrero, "A Multiagent-Based Consensus Algorithm for Distributed Coordinated Control of Distributed Generators in the Energy Internet," *IEEE Trans. Smart Grid*, vol. 6, no. 6, pp. 3006-3019, Nov. 2015.

[28] M. S. Sadabadi, Q. Shafiee and A. Karimi, "Plug-and-Play Robust Voltage Control of DC Microgrids," *IEEE Trans. Smart Grid*, vol. 9, no. 6, pp. 6886-6896, Nov. 2018.

[29] M. B. Ha, M. B. Chu and V. Sreeram, "Comparison between balanced truncation and modal truncation techniques for linear state-space symmetric systems," *IET Control Theory Applic.*, vol. 9, no. 6, pp. 900-904, 13 4 2015.

[30] S. Gugercin, R.V. Polyuga, Christopher Beattie, A. van der Schaft, "Structure-preserving tangential interpolation for model reduction of port-Hamiltonian systems," *Automatica*, vol. 48, no. 9, pp. 1963-1974, Sept 2012.

[31] R. Wang, Q. Sun, W. Hu, Y. Li, D. Ma and P. Wang, "SoC-based Droop Coefficients Stability Region Analysis of the Battery for Stand-alone Supply Systems with Constant Power Loads," *IEEE Trans. Power Electron.*, doi: 10.1109/TPEL.2021.3049241.

Wang Rui received the B.S. degree in electrical engineering and automation in 2016 from Northeastern University, Shenyang, China, where he is currently working toward the Ph.D. degree in power electronics and power drive. Since 2019, he has become a visiting scholar with the Energy Research Institute, Nanyang Technological University, Singapore. He has authored or coauthored over 40 papers, authorized over 10 invention patents. His research interest focuses on modeling of distributed renewable energy source in microgrid, stability analysis approach and stabilizing control strategy for microgrid, smart grid and so on.

Sun Qiuye (M'11-SM'19) received the Ph.D. degree in control science and engineering from Northeastern University, Liaoning, China in 2007. He is currently a full Professor with Northeastern University. He has authored or coauthored over 200 papers, authorized over 100 invention patents, and published over 10 books or textbooks. He is an *IET Fellow* and an Associate Editor of *IEEE Transactions on Neural Networks and Learning Systems*, *IET Cyber-Physical Systems*, *CSEE Journal of Power and Energy Systems*, *IEEE/CAA Journal of Automatica Sinica*, *International Transactions on Electrical Energy Systems* and so on. His current research interests include optimization analysis technology of power distribution network, network control of Energy Internet, Integrated Energy Systems and Microgrids.

Tu Pengfei (S'14-M'19) received the B.Eng. degree in electrical engineering from Wuhan University, Wuhan, China, in 2013, the M.Sc. and Ph.D. degree in power engineering from Nanyang Technological University, Singapore, in 2014, 2019 respectively. He is currently working in Energy Research Institute @ Nanyang Technological University (ERI@N) as a postdoctoral research fellow. His current research interests include reliability of multilevel converters, model predictive control, and wireless power transfer.

Jianfeng Xiao received the B.Sc. degree (with first-class honor) in School of Mechanical and Aerospace Engineering from Nanyang Technological University (NTU), Singapore, in 2011, and PhD degree in Power Engineering division, School of Electrical and Electronic Engineering, NTU, Singapore. Upon graduation, he has joined the Energy Research Institute @ NTU (ERI@N), Singapore as a post-doctor Research Fellow (RF) in Dec 2015. Currently, he is an Assistant Professor in the Newcastle University in Singapore (NUIS).

Gui Yonghao (S'11-M'17-SM'20) received the B.S. degree in automation from Northeastern University, Shenyang, China, in 2009. He received the M.S. and Ph.D. degrees in electrical engineering from Hanyang University, Seoul, South Korea, in 2012 and 2017, respectively. From February 2017 to November 2018, he worked with the Department of Energy Technology, Aalborg University, Aalborg, Denmark, as a Postdoctoral Researcher. Since December 2018, he has been working with the Automation & Control Section, Department of Electronic Systems, Aalborg University, Aalborg, Denmark, where he is currently an Assistant Professor. His research interests include control of Power Electronics in Power Systems, Energy Internet, and Smart Grids. Dr. Gui serves as an Associate Editor for the *IEEE Access* and the *International Journal of Control, Automation and Systems*. He was a recipient of the IEEE Power and Energy Society General Meeting Best Conference Paper Award in 2019.

Wang Peng (F'18) received the B.Sc. degree in electronic engineering from Xian Jiaotong University, Xian, China, in 1978, the M.Sc. degree from Taiyuan University of Technology, Taiyuan, China, in 1987, and the M.Sc. and Ph.D. degrees in electrical engineering from the University of Saskatchewan, Saskatoon, SK, Canada, in 1995 and 1998, respectively. Currently, he is a full Professor with the School of Electrical and Electronic Engineering at Nanyang Technological University, Singapore. He is an Associate Editor or Guest Editor-in-Chief of *IEEE Transactions on Smart Grid*, *IEEE Transactions on Power Delivery*, *Journal of Modern Power Systems and Clean Energy*, *CSEE Journal of Power and Energy Systems*, and so on. His current research interests include power system planning and operation, renewable energy planning, solar/electricity conversion system and power system reliability analysis.